HIGH ENERGY NEUTRON-NUCLEUS TOTAL CROSS SECTIONS

HIGH ENERGY NEUTRON-NUCLEUS TOTAL CROSS SECTIONS WITH INELASTIC SHIELDING

by

David M. Diamond

A thesis submitted to the Faculty of Graduate Studies and Research in partial fulfillment of the requirements for the degree of Master of Science.

Department of Physics
McGill University
Montreal

1977

ABSTRACT

We investigate the effect of inelastic shielding on neutron-nucleus total cross sections at high energy. Our calculations are performed within the framework of the Bochmann-Margolis coupled channel optical model formalism. In addition to the elastic channel, we consider the effect upon the total cross section of diffractively produced nucleon resonances. In particular we examine different models, inspired by triple Regge theory, for the strengths with which these resonance channels are coupled to each other. We conclude that, up to the energies considered to date, the data are consistent with a model in which the various inelastic diffractive channels are completely decoupled.

Résumé

Utilisant le formalisme du modèle optique à canaux couplés de Bochmann et Margolis, nous avons étudié l'effet d'écran formé par les canaux inélastiques sur les sections efficaces totales dans les collisions neutron-noyau à hautes énergies. Seuls le canal élastique et les canaux inélastiques diffractifs avec production de résonances du nucléon ont été considérés. La force de couplage entre les canaux inélastiques a été calculée de différentes manières, toutes inspirées de la théorie du "triple Regge". Il appert que les données expérimentales disponibles à présent sont compatibles avec un modèle dans lequel les divers canaux inélastiques diffractifs sont totalement découplés.

****

ACKNOWLEDGEMENTS

To begin with I would like to thank my supervisor Professor B. Margolis for suggesting this research to me, and for his continued guidance through the course of this work. I am particularly grateful for his accurate insights and the immense patience he displayed through the numerous ups and downs we experienced.

This research would have been completely impossible without the assistance of the McGill Computing Centre in providing computer time. I would also like to acknowledge the help of the McGill School of Computer Science and Mr. P. Desmier in providing additional computer time.

In a more personal vein I wish to thank each and every member of the Institute of Theoretical Physics at McGill from the secretaries and graduate students to the research associates and academic staff, for their warm friendship and good humour. In particular I would like to thank my former office-mate Dr. Nathan Weiss for many helpful discussions, and for his constant encouragement which was even more helpful. I would also like to thank Dr. Jim Kasman for his helpful comments regarding this research. Finally it is a pleasure for me to thank Professor W.O.J. Moser of the McGill Mathematics Department for his innumerable courtesies which I can never adequately repay.

TABLE OF CONTENTS

CHAPTER 1

Introduction

As the title of the thesis suggests, we are interested in calculating total cross sections of high energy neutrons on nuclei. In performing such a calculation, one finds it most convenient to calculate forward elastic scattering amplitudes and make use of the optical theorem to get the total cross section. This strategy enables one to ignore the numerous inelastic reactions which, if had to be calculated one by one (especially at high energy) would make the problem completely intractable.

Standard Glauber multiple scattering theory enables one to calculate the forward elastic scattering amplitude by taking into account such processes as shown in Figure 1. Figure 1(a) shows the case of single scattering, while 1(b) shows double or 2-step scattering. The "x" denotes the position where the incident neutron elastically scatters off one of the nucleons in the nucleus. This formalism however does not account for 2-step regeneration as shown in Figure 2. At sufficiently high energies the incident neutron can be inelastically converted in the nucleus into some other particle which itself then inelastically scatters back into a neutron; the incident neutron is said to have been regenerated.

This regeneration of neutrons makes the nucleus seem less "black", or less absorbing than one would expect if one did not consider this process. The difference between total cross sections calculated with and without regeneration is called the inelastic screening contribution Δ_{INEL}. The purpose of this thesis is to calculate total neutron cross sections on heavy nuclei taking this effect into account. In particular we examine different models for the strength with which the intermediate particles transform amongst themselves.

In Chapter 2 we give a more detailed explanation of inelastic screening, and describe the Bochmann-Margolis coupled channel optical model formalism which is used to calculate total neutron cross sections, taking account of inelastic screening.

In Chapter 3 we review the history of inelastic screening calculations, and recent developments in the use of the Bochmann-Margolis formalism. In particular we discuss a number of models for the 2-body forward amplitudes which couple the various intermediate states indicated in Figure 2. We also discuss other terms which appear in the equations of Chapter 2.

In Chapter 4 we describe the computer program which was written to perform the calculation of total neutron cross sections. We discuss the numerical algorithms used and the various errors present in the calculation. Finally we present the results of our calculations along with the available experimental data.

In appendix A we present Bochmann's derivation of the equivalence of the eikonal solution of the coupled channel optical model to a Glauber-type multiple scattering model. This is a relevant calculation, but somewhat off the main line of the thesis, and so has been put in an appendix.

CHAPTER 2

Theory

2.1 Screening

We begin with a qualitative wave-mechanical picture of elastic and inealstic screening.[1]

Consider a plane wave incident on a nucleus as in Figure 3. The incident wave scatters off the nucleons at the front of the nucleus. The part of the plane wave which is scattered gives rise to spherical wavelets coming off the target nucleons. The incident plane wave then interferes with the forward scattered wavelets in just such a fashion so as to account for the particles scattered out of the beam. This is essentially the physical statement of the optical theorem. This interference caused by the outer nucleons clearly reduces the amplitude of the incident plane wave so that the nucleons at the back of the nucleus are in effect shadowed or screened, and do not contribute as much to the total cross section as do the outer nucleons facing the beam.

Now suppose we consider production on a nucleon to a given final state; how is this affected by screening? Consider a nucleon X as shown in Figure 3. Production to a given final state Y may proceed in two ways. In both cases we want the nucleus to serve only as a passive target for our incident beam (recall we want to calculate ELASTIC scattering amplitudes to get the total cross section), and so we require that no interaction with a target nucleon be sufficiently strong to excite it into a higher energy level (In practice the energy levels of nucleons appear degenerate at high energies, so in reality the most stringent condition we can impose is that the incident beam particle not knock a nucleon out of the nucleus, or cause the nucleus to break up.)

In the first process the incident wave may strike X and produce the state Y directly (process (1)). Or, the incident wave may scatter off one of the nucleons in front of X, and then the scattered wave produces the state Y on X (process (2)). If, as we just said, no target excitation occurs then the two final quantum states are identical, and must be summed coherently. The phase of (2) relative to (1) is given by the forward elastic scattering amplitude on the nucleon multiplied by a factor to account for the propogation between nucleons. The forward elastic scattering amplitude is predominantly imaginary (especially at high energy) and by the optical theorem is positive, so this contributes a factor +i. The classical reconstruction of a wavefront from a plane of scatterers also gives a factor +i (the propogation factor) so this means that (2) is out of phase with (1) by approximately 180°, and they interfere destructively. Thus as we would expect the shadowing, or screening, reduces the cross section for the production of the state Y on the nucleon X.

So far this can all be described by standard Glauber theory. However, at sufficiently high energy the secondary wavelets in process (2) do not have to be identified with the original beam particles; they may be diffractively produced resonances. We shall define what we mean by "diffractive production"more precisely later, but for the moment we shall only mention that resonances which are diffractively produced have the identical quantum numbers as the incident beam, except possibly for spin and parity. This makes it possible for such particles.

a) to be produced on a nucleon without disturbing it too much, and

b) to interfere with the original beam.

Clearly if this mechanism exists we must include it in our calculations in order to make accurate theoretical predictions.

The method by which we include these diffractively produced intermediate states is the coupled channel optical model of Bochmann and Margolis.(2) This model requires the solution of a simultaneous set of wave equations. Each wave equation describes the propogation of one type of particle through the nucleus. The equations are coupled to each other by optical potentials which allow one channel either to elastically scatter or inelastically scatter into another channel.

2.2 The Coupled Channel Formalism.

In this section we present a derivation of the Bochmann-Margolis coupled channel optical model. In Appendix A we demonstrate the equivalence of this with a Glauber-type multiple scattering model.

2.2.1 We list here the approximations which we make in deriving this model:

(i) We solve the equations in the eikonal approximation. This reduces them from second order differential equations to equations of first order which are easier to deal with. This is a good approximation at high energies for small angle scattering.

(ii) Since we are dealing primarily with diffractive reactions we neglect their dependence on isospin. That is, we assume that the isospin nonflip amplitute dominates. We do the same for ordinary spin, but with somewhat less justification - see the discussion in Section 3.2.4.

(iii) We describe the nuclear target ground state by a product of single particle wave functions. Thus we ignore the effect upon the reaction of correlations between the target nucleons. At the high energies we are considering this is a good approximation.

(iv) We make a large A (atomic number) approximation. This can be clearly seen in the derivation in Appendix A. This approximation is well satisfied for medium and heavy nuclei.

2.2.2 We introduce a channel α incident on a nucleon in the nucleus and describe elastic scattering and coherent production by the coupled wave equation:

$$(1)\quad (\nabla^2 + p_\alpha^2)\,\psi_\alpha(\vec{r}) = \sum_{\alpha'} U_{\alpha'\alpha}(\vec{r})\,\psi_{\alpha'}(\vec{r})$$

where ψ_α is the wave function of the particle incident on the nucleon,

$\psi_{\alpha'\neq\alpha}$ are the wave functions for the channels which are coupled coherently to the channel α (the summation over the channels α' in Equation (1) includes the term $\alpha = \alpha'$ which is the term for elastic scattering of the incident channel),

$p_\alpha = \sqrt{E^2 - m_\alpha^2}$ is the magnitude of the 3-momentum of the channel α having mass m_α, where E is the total energy of the incident particle in the lab,

$U_{\alpha'\alpha}$ are optical potentials; $U_{\alpha\alpha}$ is the optical potential for elastic scattering in the channel α (the presence of the forward elastic scattering amplitude in $U_{\alpha\alpha}$ means, by the optical theorem, that it also accounts for damping of the wave in the nucleus) and $U_{\alpha'\alpha}(\alpha \neq \alpha')$ is the optical potential for coherent production of the channel α by the presence of channel α'. We assume $U_{\alpha'\alpha} = U_{\alpha\alpha'}$.

The optical potentials are given by[3]

$$(2)\qquad U_{\alpha'\alpha}(\vec{r}) = -2i\, p_\alpha\, A \int d^2b'\, \rho(\vec{b}',z)\Gamma_{\alpha'\alpha}(\vec{b}-\vec{b}')$$

$\vec{r}$ is a 3-dimensional position vector with the origin at the centre of the nucleus; we denote the magnitude of the vector $\vec{r}$ by r (similarly for other vectors).

z is the z-component of $\vec{r}$ and we assume that this is parallel to the incident beam in the lab.

$\vec{b}$ is the 2-dimensional component of $\vec{r}$ in the plane perpendicular to z, i.e. the impact parameter; the integration in Equation (2) is over the range of impact parameters in the nucleus.

A is the number of nucleons in the nucleus.

$\rho(\vec{b},z) = \rho(\vec{r})$ is the nuclear density function normalized to unity.

$\Gamma(\vec{b}-\vec{b}')$ is the so-called "profile function" of a 2-body interaction and is given by

$$(3)\qquad \Gamma_{\alpha'\alpha}(\vec{b}) = \frac{1}{2\pi i\, p_\alpha} \int d^2q_\perp\, f_{\alpha'\alpha}(\vec{q}_\perp)\, e^{-i\vec{q}_\perp\cdot\vec{b}}$$

where $\vec{q}_\perp$ is the transverse momentum transfer between the channels α and α' (i.e. $q_\perp = (\vec{p}_{\alpha'}-\vec{p}_\alpha)\cdot\vec{b}$), and

$f_{\alpha'\alpha}(\vec{q}_\perp)$ is the 2-body amplitude for the coherent production of the channel α by the channel α' incident on a nucleon.

We see that the 2-body profile function is just the 2-dimensional Fourier transform of the 2-body scattering amplitude.

Taking the inverse transform we have :

(4) $$f_{\alpha'\alpha}(\vec{q}_\perp) = \frac{ip_\alpha}{2\pi} \int d^2b \, \Gamma_{\alpha'\alpha}(\vec{b}) e^{i\vec{q}_\perp \cdot \vec{b}}$$

and

(5) $$f_{\alpha'\alpha}(0) = \frac{ip_\alpha}{2\pi} \int d^2b \, \Gamma_{\alpha'\alpha}(\vec{b}).$$

Now if we assume that $\rho(\vec{r})$ is slowly varying inside the nucleus we may pull it out of the integral in Equation (2) and we then have

$$U_{\alpha'\alpha}(\vec{r}) = -2ip_\alpha A\rho(\vec{r}) \int d^2b' \, \Gamma_{\alpha'\alpha}(\vec{b}-\vec{b}')$$

(6) or

$$U_{\alpha'\alpha}(\vec{r}) = -4\pi A\rho(\vec{r}) \, f_{\alpha'\alpha}(0) \quad \text{by Equation (5).}$$

We shall refer to $f_{\alpha'\alpha}(0)$, or more simply just $f_{\alpha'\alpha}$ as the forward scattering amplitude.

To solve Equation (1) we use the eikonal approximation, which, as we said, is a good approximation at high energies. Essentially it assumes that a high energy particle traversing a (finite) potential will not be deflected greatly by the potential. That is, the wave function ψ will differ from the incident wave e^{ipz} by a term that varies slowly over distances of the order $1/p(\sim V)$. In this spirit we make the substitution

(7) $$\psi_\alpha(\vec{r}) = e^{ip_\alpha z} \phi_\alpha(\vec{r})$$

where $\phi_\alpha(\vec{r})$ is slowly varying. Putting this into Equation (1) and taking $e^{ip_\alpha z}$ to the right hand side ... get

$$(8) \qquad \nabla^2\phi_\alpha(\vec{r}) + 2ip_\alpha \frac{\partial\phi_\alpha(\vec{r})}{\partial z} = \sum_{\alpha'} U_{\alpha'\alpha}(\vec{r})e^{i(p_{\alpha'}-p_\alpha)z}\phi_{\alpha'}(\vec{r})$$

By our hypothesis we may neglect $\nabla^2\phi_\alpha(\vec{r})$, and our problem reduces to the solution of a coupled set of linear, first order, complex differential equations:

$$(9) \qquad \frac{\partial\phi_\alpha(\vec{r})}{\partial z} = \frac{1}{2ip_\alpha} \sum_{\alpha'} U_{\alpha'\alpha}(\vec{r})e^{i(p_{\alpha'}-p_\alpha)z}\phi_{\alpha'}(\vec{r})$$

The boundary condition for Equation (9) is determined by the assumption that before the beam strikes the nucleus only the incident channel α_o is present so

$$(10) \qquad \phi_\alpha(\vec{b},z = -\infty) = \delta_{\alpha\alpha_o}.$$

We see that with this assumption we neglect backscattering, which again is a good approximation at high energy.

We note that if we re-write equation (9) in terms of $\psi(\vec{r})$, it is directly integrable if $U_{\alpha'\alpha}(\vec{r})$ is independent of $\vec{r}$. From Equation (6) we see this is true if $\rho(\vec{r})$ is a constant. We prefer however to use a Woods-Saxon density distribution (see Section 3.4) because it is a better approximation.

2.2.3 At this point we should discuss the coherence requirement. As mentioned in Section 2.1 we require that in scattering off a target nucleon the incident neutron must not disturb it too violently. Now in an inelastic collision at high energy, where the neutron converts into a higher mass resonance, there is a minimum forward momentum transfer due to the mass difference. This has the form

$$(11) \qquad p_{\alpha'} - p_{\alpha} = \frac{m_{\alpha}^2 - m_{\alpha'}^2}{p_{\alpha'} + p_{\alpha}} .$$

Production of the state α' by the state α will be coherent over the whole nucleus only if $(p_{\alpha'} - p_{\alpha})z$ is sufficiently small that $e^{i(p_{\alpha'}-p_{\alpha})z}$, which appears in Equation (9), does not oscillate significantly. Otherwise this term will give rise to large cancellations.

It is thus reasonable that the coherence requirement be

$$(12) \qquad (p_{\alpha'} - p_{\alpha})R << 1$$

where R is the radius of the nucleus.

However, in performing numerical calculations the very presence of the exponential serves to enforce coherence automatically. Whenever the momentum transfer is too large the oscillations cause the contribution for that momentum transfer to cancel (approximately). So for this work the coherence requirement is not a stringent condition.

2.2.4 We now proceed to use the equations we have derived to calculate the elastic scattering amplitude, which will in turn give us the total cross section.

In elementary scattering theory[4] we calculate the Green's function for the Schroedinger equation and transform it into an integral equation having the form

$$\psi(\vec{r}) = \psi_o(\vec{r}) + \frac{e^{ipr}}{r} f(\vec{p}).$$

where $$f(\vec{p}) = -\frac{1}{4\pi} \int d^3r\, e^{-i\vec{p}\cdot\vec{r}}\, U(\vec{r})\, \psi(\vec{r}),$$

$\psi(\vec{r})$ is the scattered wave, and

$\psi_o(\vec{r})$ is the incident wave.

(Note that we have written the Schroedinger equation in the form $\nabla^2\psi(\vec{r}) + p^2\psi(\vec{r}) = U(\vec{r})\psi(\vec{r})$.)

Extending this procedure to our coupled wave equations we see that

$$(13) \qquad f_{\alpha_o\alpha}(\vec{p}_\alpha) = -\frac{1}{4\pi} \int d^3r\, e^{-i\vec{p}_\alpha\cdot\vec{r}} \sum_{\alpha'} U_{\alpha'\alpha}(\vec{r})\psi_{\alpha'}(\vec{r})$$

where $f_{\alpha_o\alpha}(\vec{p}_\alpha)$ is the coherent amplitude for the channel α_o to scatter off a nucleus into the channel α .

Now when $\vec{p}_{\alpha_o}$ is along the z-axis, and the scattering angle and momentum transfer are small, we may approximate $\vec{p}_\alpha$ by

$$\vec{p}_\alpha \approx [(\vec{p}_\alpha - \vec{p}_{\alpha_o})\cdot\hat{b}]\,\hat{b} + P_\alpha\hat{z}$$

where "^" represents a unit vector. That is, the longitudinal component of $\vec{p}_\alpha$ is approximately equal to p_α , and the transverse component is approximately equal to the momentum transfer. If $\vec{p}_\alpha - \vec{p}_{\alpha_o} = \vec{q}_\alpha$ then

$$f_{\alpha_o\alpha}(\vec{p}_\alpha) = -\frac{1}{4\pi}\iint d^2b\,dz\; e^{-\vec{q}_\alpha\cdot\vec{b}}\; e^{-ip_\alpha z} \sum_{\alpha'} U_{\alpha'\alpha}(\vec{r})\,\psi_{\alpha'}(\vec{r})$$

With

$$\psi_\alpha(\vec{r}) = e^{ip_\alpha z}\, \phi_\alpha(\vec{r})$$

$$f_{\alpha_o\alpha}(\vec{p}_\alpha) = -\frac{1}{4\pi}\int d^2b\; e^{-i\vec{q}_\alpha\cdot\vec{b}} \int_{-\infty}^{\infty} dz \sum_{\alpha'} e^{i(\vec{p}_{\alpha'}-\vec{p}_\alpha)z}\; U_{\alpha'\alpha}(\vec{r})\;\phi_{\alpha'}(\vec{r})$$

By Equation (9) and (10) $= -\frac{1}{4\pi}\int d^2b\; e^{-i\vec{q}_\alpha\cdot\vec{b}} \int_{-\infty}^{\infty} dz\; 2ip_\alpha \frac{\partial}{\partial z}\phi_\alpha(\vec{r})$

(14) $$f_{\alpha_o\alpha}(\vec{p}_\alpha) = -\frac{ip_\alpha}{2\pi}\int d^2b\; e^{-i\vec{q}_\alpha\cdot\vec{b}}\; [\phi_\alpha(\vec{b}, z=\infty) - \delta_{\alpha\alpha_o}]$$

In the forward direction the component of $\vec{q}_\alpha$ parallel to $\hat{b}$ (the transverse momentum transfer) is zero, and the elastic scattering amplitude is given by

(15) $$f_{\alpha_o\alpha_o}(0) \equiv f_{\alpha_o\alpha_o} = -i\, p_{\alpha_o}\int_0^\infty db\; b\; [\phi_{\alpha_o}(b, z=\infty) - 1]$$

where we have assumed azimuthal symmetry.

Finally then, by the optical theorem, we have the total cross section :

$$(16) \qquad \sigma_{ToT} = \frac{4\pi}{P_{\alpha_o}} \quad \text{Im} \quad f_{\alpha_o \alpha_o} = 4\pi \int_0^{\infty} db\; b \; [1 - \text{Re}\; \phi_1(b,\infty)]$$

To calculate the total cross section we have written a computer program which solves Equation (9) for $\phi_1(b,\infty)$, and then performs the integration in Equation (16). We describe the program in Chapter 4.

CHAPTER 3

Historical Review, Forward Amplitudes, and Nuclear Parameters.

Of utmost importance in the Bochmann-Margolis formalism are the forward amplitudes $f_{\alpha'\alpha}$ which serve to couple the various channels. Before discussing these forward amplitudes it would be appropriate and convenient to review the historical situation ; this will show us the source for a number of models for the $f_{\alpha'\alpha}$ and help put our calculation into context.

3.1 History.

As explained in Section 2.1 there are two kinds of shadowing corrections to neutron total cross sections on nuclei. First is the elastic shadowing which is accounted for in Glauber theory. Second is the inelastic shadowing. This was first discussed in 1966 in a paper by Abers, Burkhardt, Teplitz, and Wilkin[(5)]. The first optical model treatment of the problem was by Pumplin and Ross[(6)] in 1968. In 1969 Gribov[(7)] performed a similar analysis using the graph technique. Pumplin and Ross performed some numerical calculations of the inelastic shadowing correction Δ_{INEL}, but rather than considering only diffractively produced intermediate states (as we have indicated in Section 2.1 this should be the case) they included all kinematically allowed masses.

This was done by looking at the so-called one-particle inclusive reaction $p + p \rightarrow p + X$ where X can be anything allowed by the various conservation laws. In this kind of experiment only the final-state proton is detected and momentum-analyzed. The mass of whatever comprises X is hence referred to as the "missing mass". The kinematical variables in such an experiment are the usual Mandelstam variables and the invariant missing mass. These are defined as follows. For the experiment

$$a + b \rightarrow p + X$$

we have

$$s = (P_a + P_b)^2$$

$$t = (P_a - P_p)^2$$

$$u = (P_b - P_p)^2$$

where P_a denotes the 4-vector $(E_a, \vec{p}_a)$ and our metric is such that $P_a^2 = E_a^2 - |\vec{p}_a|^2 = m_a^2$. The invariant missing mass is given by

$$M^2 = s+t+u-m^2_a - m^2_b - m^2_p$$

$$= (P_a + P_b - P_p)^2 .$$

At the energies we are considering we regard the proton and the neutron as equivalent, so a study of $p + p \rightarrow p + X$ also gives the amplitudes for a neutron to strike a nucleon and turn itself into some higher mass state.

As we have said, Pumplin and Ross included the whole missing mass spectrum as possible intermediate states in neutron regeneration. At low energies this had the effect of depleting total cross sections by as much as 20%, and this was too large-they obtained too much inelastic shielding.

In 1973 Kaidalov and Kondratyuk[8] proposed that only the diffractive part of the missing mass spectrum contributes to the inelastic shadowing effect. By a diffractive reaction we mean one that proceeds by exchange of vacuum quantum numbers in the t-channel, i.e. pomeron exchange. Two-body diffractive reactions are readily identified by having a weak energy dependence in $\frac{d\sigma}{dt}$, and having amplitudes which are mostly imaginary. Of greatest interest are elastic scattering and diffraction dissociation at high energy. Diffraction dissociation reactions are quasi two-body reactions of the sort

$$p + p \to p + N^*$$

where N^* is some nucleon resonance having the same quantum numbers as the nucleon (except possibly spin and parity) but higher mass. The expectation is that as two-body reactions are made at ever higher energies, only these diffractive reactions will persist as the energy goes to infinity.

Kaidalov and Kondratyuk pointed out that in considering mechanisms for Δ_{INEL}, only diffraction dissociation has an imaginary amplitude as required for the proper sign of the correction term (recall discussion of Section 2.1). They separate the total inelastic cross section for $p + p \to p + X$

into two parts, the diffractive part and the inelastic background. The inelastic background may be viewed at low energy as the result of non-vacuum Regge exchanges, such as ω, ρ, A_2 and π. Because of the difference in phase between these exchanges and pomeron exchange, Kaidalov and Kondratyuk felt that these two contributions to Δ_{INEL} should be examined separately. In a Regge-pole framework they showed that the contribution of the inelastic background to Δ_{INEL} was negligible compared to the contribution of diffraction dissociation.

In 1973 Karmanov and Kondratyuk[9] performed a calculation of Δ_{INEL} using only the contribution of diffraction dissociation. They did their calculation to second order in perturbation theory. This means that they allow for only one transition from a neutron to a resonance then back to a neutron. Only the inelastic couplings are calculated to second order; elastic scatterings are treated to all orders (i.e. any number of elastic scatterings are allowed). (We note here that our coupled-channel calculation is done to all orders in the inelastic couplings. The fact that we describe the reaction by coupled equations means that any number of back and forth transitions can occur between all channels.) Karmanov and Kondratyuk found that inclusion of Δ_{INEL} gave a 2-3% decrease in total neutron cross sections above 10 gev/c, and that Δ_{INEL} increases logarithmically with energy.

In 1975 Murthy et al.[10] reported results of high energy (30-300 gev/c) total neutron-nucleus cross section measurements performed at Fermilab. In analyzing their results they used the method of Karmanov and Kondratyuk to calculate Δ_{INEL}. Although the error bars on their measurements made precise comparisons difficult, the inclusion of Δ_{INEL} brought the theoretical curve into good agreement with the experimental points, particularly in the energy dependence of the data.

3.2 Recent Developments and the Inter-Resonance Couplings

3.2.1. Late in 1975 a criticism of the analysis of Murthy et al. was published by D. Julius[11]. His work revealed very little inelastic shielding, and he felt that if the experimentalists had used different nuclear radii they would have found virtually no inelastic shielding at all. Julius used the Bochmann-Margolis coupled channel formalism. To do this he had to specify the forward amplitudes $f_{\alpha'\alpha}$. This he did as follows:

Triple Regge theory[12] predicts the cross section for $p + p \to p + X$ to be

$$\left.\frac{d^2\sigma}{dt\, dM^2}\right|_{t=0} = c/M^2 \tag{15}$$

where Julius, following Fishbane and Trefil[13] takes the value of c to be 2.9 mb/gev^2. At high energy the scattering amplitude is related to $\frac{d\sigma}{dt}$ by

$$\frac{d\sigma}{dt} = \frac{\pi}{p^2} |f|^2 \tag{16}$$

If we assume that the phase is purely imaginary then the amplitude for production of some channel j by an incident neutron (in channel 1) is given by

$$f_{1j} = i\, p_1 \left(\frac{1}{\pi} \frac{d\sigma}{dt} (1 \to j)\right)^{1/2} \tag{17}$$

Now the missing mass spectrum is given by $\left.\frac{d^2\sigma}{dt\, dM^2}\right|_{t=0}$ vs. M^2. If we divide this into intervals of δM^2, where the j th channel is represented by the j th mass interval, we may integrate the spectrum approximately to obtain

$$\left.\frac{d\sigma}{dt}(1 \to j)\right|_{t=0} = \left.\frac{d^2\sigma}{dt\, dM^2}\right|_{\substack{t=0\\ M^2=M^2_j}} \delta M^2 \tag{18}$$

$$= \frac{c}{M^2_j}\, \delta M^2 \tag{19}$$

(In particular Julius used $\delta M^2 = m^2_N$ where m_N is the mass of the nucleon, and $M^2_j = j\, m^2_N$, so $\left.\frac{d\sigma}{dt}(1 \to j)\right|_{t=0} = c/j$. We will use a varying mass interval and so we leave the equations in the form given)

To get the further amplitudes $f_{ij} (i,j \neq 1)$ Julius made what he felt was the simplest possible generalization of Equation (19), namely,

$$\left.\frac{d\sigma(i \to j)}{dt}\right|_{t=0} = \left(\frac{c}{|M_i^2 - M_j^2| + m_N^2}\right) \delta M^2 \qquad (20)$$

(This generalization is more apparent using Julius's choice $\delta M^2 = m_N^2$. Then $\left.\frac{d\sigma(i \to j)}{dt}\right|_{t=0} = \frac{c}{|i-j| + 1}$)

With the assumption of imaginary phases we get

$$f_{ij} = i\, p_i \left(\frac{c}{\pi} \frac{\delta M^2}{|M_i^2 - M_j^2| + m_N^2} \right)^{1/2} \qquad (21)$$

The neutron 2-body inelastic scattering amplitude f_{11} is obtained from pp elastic scattering data, and all resonance elastic scattering amplitudes f_{jj} are set equal to f_{11}.

Julius used a coherence condition based on Equation (12) to cut off the missing mass spectrum. Up to 60 gev/c he was able to use the Bochmann-Margolis formalism, since at this energy only a comparatively small number of coupled channels was required. The computer time necessary to solve the coupled channel problem rises very rapidly with the number of coupled channels, and so Julius devised a high energy approximation to get to neutron momenta above 60 gev/c. The details are contained in reference (11).

3.2.2. In what follows we shall have a number of comment to make concerning Julius's paper. The first and most important, which we shall make now, is that there is NO JUSTIFICATION either theoretical or experimental for Julius's choice of $f_{\alpha'\alpha}$ where $\alpha \neq \alpha' \neq 1$ (in future we shall always refer to the amplitudes coupling various resonances to other resonances by $f_{\alpha'\alpha}$; we shall treat the cases of $f_{1\alpha}$ and $f_{\alpha\alpha}$ separately). His choice of amplitudes is little more than a guess, and as we shall see, other generalizations of the triple Regge formula are possible. Since it seems unlikely that there will ever be direct experimental evidence to guide us in this matter the best that we can hope to do in the framework under discussion is to try different forms for the $f_{\alpha'\alpha}$ and see which fit the data best.

3.2.3. The previous comment and others are contained in a reply to Julius's criticism by Ayre and Longo[14]. The crucial point they raise is that the triple Regge formula Julius uses for direct resonance production by a neutron(f_{1j}) simply does not agree with the data. Recall that these amplitudes may be reconstructed from the missing mass spectrum by dividing it into bins, and taking the area under the curve for each bin. The amplitude f_{1j} is proportional to the area of the j th bin. We recall too that we must consider only the diffractive part of $\frac{d^2\sigma}{dt\,dM^2}$. In their calculation Kaidalov and Kondratyuk had to extrapolate the data then available ($E_{LAB} \gtrsim 30$ gev) to infinite energy to obtain the diffractive part. The experimentalists in reference (10) note that in the Fermilab data $\frac{d^2\sigma}{dt\,dM^2}$ at small t becomes approximately energy independent for $E_{LAB} \gtrsim 50$ gev. From this they conclude that the high energy limit has been reached, and assume that the whole (forward) missing mass spectrum is diffractive in nature. The formula used by Murthy et al. to fit the data is

$$\frac{d^2\sigma}{dt\, dM^2}\bigg|_{t=0} = 26.47(M^2-1.17)-35.969(M^2-1.17)^2+18.47(M^2-1.17)^3$$

$$- 4.13(M^2-1.17)^4+.341(M^2-1.17)^5 \quad \text{for } 1.17 < M^2 < 5 \text{ gev}^2$$

$$= 4.4/M^2 \qquad \text{for } M^2 > 5 \text{ gev}^2 \ . \tag{22}$$

Figure 4 shows the comparison between this formula and that used by Julius. The discrepancy between Julius and Murthy et al. becomes immediately clear. In the coupled channel formalism the f_{1j}'s are the parameters which couple the neutron to the diffractive resonance. The f_{1j}'s are proportional to the area under the curve $\frac{d^2\sigma}{dt\, dM^2}\big|_{t=0}$. From Figure 4 we see that the area under Julius's form for $\frac{d^2\sigma}{dt\, dM^2}\big|_{t=0}$ is much less than for the form used by Murthy et al., which is a fit to the data. This means that in Julius's calculation the neutron is much less likely to turn into a diffractive resonance and the whole regeneration effect is considerably reduced. In the limit that the f_{1j}'s are set to zero (except for j = 1) then regardless of the values of the $f_{\alpha'\alpha}$'s we completely decouple the neutron channel from all the others and the result of our calculation is just the unregenerated cross section.

3.2.4. At this point we interpose a further comment of our own. We have been discussing the missing mass spectrum $\left.\frac{d^2\sigma}{dt\, dM^2}\right|_{t=0}$. Of course t = 0 is kinematically inaccessible for $M^2 \neq m^2_N$, but in the forward direction $t = t_{min}$ is very nearly equal to zero at high energies. The point however is that measurements cannot be made at $\theta = 0$ in the beam. The t-dependence of the reaction is taken up to some limiting t value, and then is extrapolated to t = 0. There is no problem with this extrapolation if the reaction does not involve helicity flip. However if there is a helicity nonconserving component to the amplitude its t dependence includes a term $(\sqrt{-t})^{\Delta\lambda}$ where $\Delta\lambda$ is the helicity flip. Clearly this goes to zero as t goes to zero. The helicity conserving amplitude does not go to zero at t = 0.

Until recently it was thought that diffraction dissociation conserved helicity in the s-channel, following the behaviour observed in elastic scattering and vector meson photoproduction. It now appears that among diffraction dissociations vector-meson photoproduction is an exception, for all the other observed reactions do not conserve s-channel helicity.

This presents us with a problem. In extrapolating their data to t = 0 the experimentors will not have taken account of any helicity nonconserving amplitudes. If the data was taken up to a very small t-value these amplitudes will have mostly damped out, and the error will be small. If these amplitudes were large enough to give a significant contribution at the lowest t-value measured then the extrapolation to $t = 0$ will be too large. As we have seen in Section 3.2.3 this means that we will overestimate the inelastic shadowing.

Since the details of the extrapolation are not available to us, and particularly since the helicity nonconserving amplitudes in diffraction dissociation are not well known to begin with, we have essentially ignored this whole problem. If it comes to light that the missing mass spectrum has been significantly overestimated, the inelastic shadowing correction will have to be decreased appropriately.

3.2.5. Returning now to the paper of Ayre and Longo we come to their second major point, which enlarges upon the first comment we made in Section 3.2.2. They point out that not only is Julius's model for f_{ij} ad hoc, but it is designed so as to give large couplings between some of the high-mass resonances. Looking at Equation (21) we see that when M^2_i and M^2_j are close, f_{ij} gets large. Physically this is of course possible, but it is also possible that f_{ij} becomes smaller uniformly as M^2_i and M^2_j get larger. This is reflected in another generalization of the triple Regge model due to F. Henyey which Ayre and Longo quote. He finds

$$f_{ij} = i\, p_i \left(\frac{.24}{M_i\, M_j}\right)(\delta M^2)^{1/2} \tag{23}$$

In this model it is clear that there is a much weaker coupling between the high-mass states.

3.2.6. Heuristically it is interesting to note the effect on the total cross section due to changes in the various forward amplitudes. As we have already noted the inelastic shadowing is due to coupling the neutron channel to the various resonance channels. The greater the coupling, the more shadowing we get, so as the f_{1j}'s go up the total cross section goes down. However for the inter-resonance couplings the opposite is true. As the f_{ij}'s go up the total cross section goes up. This effect is less pronounced than for the f_{1j}'s and can be understood as follows.

The result of our coupled channel calculation is the neutron elastic scattering amplitude which is directly proportional to the total cross section by the optical theorem. As the neutron propogates through the nucleus its scattering amplitude is depleted by conversions to resonance states and enhanced by resonances converting back into neutrons. Now if we set the f_{ij}'s to zero, a neutron going into the j-th resonance channel can do only one of two things: either it may elastically scatter (recall $f_{jj} = f_{11}$) or it may turn itself back into a neutron. For the larger masses the elastic amplitude is much greater than the amplitude for conversion to the neutron channel (which goes as $1/M^2$ for large mass). So when the f_{ij}'s are set to zero, a neutron which goes into the j-th resonance channel will be inclined to stay there, thus depleting the neutron elastic amplitudes and lowering σ_{ToT}. On the other hand as the f_{ij}'s are made larger, the probability goes up that the j-th resonance will then convert to some other resonance which will find it easier to return to the neutron channel. Essentially more ways are open for an inelastically scattered neutron to return to the elastic channel, and so the total cross section goes up.

3.2.7. Still on the subject of the coupling of the higher mass resonances, we have assumed that the inter-resonance amplitudes f_{ij} are purely imaginary (and positive). Julius assumes the f_{1j}'s are also positive imaginary, while Ayre and Longo set the phase of the f_{1j}'s equal to the phase of f_{11}. Once again this is all pure speculation, although we would expect the amplitudes to be predominantly imaginary if they are diffractive. Nonetheless it is of interest to see what would happen to the calculated cross sections by varying the signs of the amplitudes. Remarkably enough we found (and this is easy to show) that alternating the signs of the amplitudes (so that $f_{ij} \rightarrow (-1)^{i-j} f_{ij}$) is equivalent to alternating the sign of the wavefunction in each channel ($\phi_i \rightarrow (-1)^i \phi_i$). Since the cross section is independent of the sign of the wavefunction the result is the same. Hence we would expect that if the phase varies in some random fashion the calculated cross sections will not change by much. To test the most extreme possible difference we have calculated cross sections with all non-elastic amplitudes changed in sign. The results are shown in Chapter 4.

3.3. Summary of Amplitudes

We have two models for the f_{1j}'s, the amplitudes for producing a diffractive resonance by a neutron incident on a nucleon. One is based upon a discrete approximation to the tripple Regge formula, Equation (15), used by Julius. The other, used by Ayre and Longo, is based upon a discrete approximation to the experimental data as described by Equation (22). Julius assumes the phases are positive imaginary, while Ayre and Longo assume the phases are the same as for neutron elastic scattering.

We also have two models for the inter-resonance couplings. Both are generalization of the triple Regge formula, Equation (15). The first is that of Julius, Equation (21). The second is that of Henyey, Equation (23). Both models assume the phases are positive imaginary.

The elastic amplitudes f_{jj} are all set equal to f_{11} the neutron elastic scattering amplitudes. This is obtained via the optical theorem from experimental data on pp total cross sections[15], and the phase of the forward elastic scattering amplitude [16].

On this point we issue one caveat. At low energy we are not justified in simply using nn elastic scattering. There are protons in the nucleus and the np total cross section and phase will not be the same as for nn (or pp) scattering due to different non-leading Regge exchanges. Presumably however, at higher energies these terms will become small and the error we commit in considering only nn scattering terms will become negligible.

3.4. Nuclear Parameters

We have assumed a spherical nucleus, and have chosen to use a Woods-Saxon formula for the density function. This has the form

$$\rho(r) = \frac{\rho_o}{1 + \exp(\frac{r-R}{c})} \qquad (24)$$

where R is the nuclear half-density radius

c is the nuclear "skin thickness"

and ρ_o is a normalization factor such that

$$4\pi \int_0^\infty \rho(r)dr = 1 \quad .$$

This normalization integral was calculated numerically, with the range of integration cut off at R + 16C.

Accurate measurements of the parameters R and C were made in the high statistics ρ-photoproduction experiment of Alvensleben et al.[17]. We used their value of C = .545 fm., but we modified their radius parameter slightly to account for the difference between pp scattering and γp scattering. Our modification was made as follows.

Around the energies we are considering, the differential cross section for pp scattering goes roughly as $e^{-10|t|}$ and for γp scattering goes as $e^{-8|t|}$. If we assume that the proton has a Gaussian shape as a function of impact parameter, then the differential cross section, which is the Fourier-Bessel transform of the spatial distribution, is also a Gaussian in momentum transfer, which means it is an exponential in t. To be precise, if the matter distribution is given by e^{-b/R^2} then the differential cross section is given by $e^{-R^2|t|/4}$ where R is the Gaussian radius parameter.

If R_1 is the proton's radius parameter in pp scattering and R_2 is the parameter in γp scattering then,

$$\frac{R_1^2 - R_2^2}{4} = 2 \text{ gev}^{-2}$$

$$(R_1-R_2)(R_1+R_2) = 8 \text{ gev}^{-2}$$

$$(R_1-R_2)\, 2\tilde{R} = 8/25 \text{ fm}^2$$

$$R_1-R_2 = \frac{4}{25\tilde{R}} \text{ fm}$$

where $\tilde{R}_o$ is the average proton radius. If we assume $\tilde{R}$ = 1.2 fm we get $R_1 - R_2$ = .13 fm. This is the number we added to the radius parameter of Alvensleben et al. (our radius parameter for lead is thus 6.95 fm.).

Clearly this is all very approximate. In the first place the R used above is the Gaussian parameter not the Woods-Saxon parameter. Secondly the slopes of pp and γp scattering get steeper with energy, corresponding to an increasing radius parameter. Hence to be precise we really should use an energy dependent radius. We found however that the rough treatment outlined above was sufficient over the energy range considered.

In the paper of Murthy et al. the authors use nuclear parameters which they calculate from a best fit to low energy (< 10 gev/c) total neutron cross section data (there they fit the data with a Glauber-type formula given by Franco, and they used the expression given by Karmanov and Kondratyuk for the inelastic screening). These nuclear parameters correspond precisely to the ones we require and do not need to be altered as above. Unfortunately however we found that using these values in our coupled channel formalism we underestimated the total neutron cross section at all energies.

CHAPTER 4

The Calculation-Results and Discussion

4.1 The Calculation

Our contribution to the understanding of the inelastic shadowing correction to total neutron-nucleus cross sections is presented in this chapter. We calculated total neutron cross sections on lead for all the models presented in Chapter 3, using the formalism of Chapter 2. Several of these calculations were never done before. We limit our investigation to lead mainly because of the limited computing funds available. The calculation however is easily extended to other large A nuclei.

4.1.1. We have written a computer program to perform the calculations shown in Chapter 2. Specifically we integrate Equation 16 numerically using the method of Romberg Extrapolation of the trapezoid rule[18]. As in the calculation of ρ_o for Equation 24 we cut off the integration at $b = R + 16C$. In doing the numerical integration the program evaluates the integral at a number of values of the impact parameter b. For each evaluation of the integrand the program must solve the coupled set of differential equations shown in Equation 9 along with the boundary condition given in Equation 10. We solve this coupled set of equations using a fourth order Runge-Kutta method[18].

4.1.2. In Section 4.1.3 we list all of the models for which we have performed calculations. For all these models we have calculated total neutron cross sections on lead from $p_{LAB}=5$ gev/c to 400 gev/c. In all the models considered the missing mass spectrum was cut off by the coherence condition given by Julius, namely

$$\frac{m^2 - m_N^2}{2\ E_{LAB}} \leq \frac{3}{R'}$$

where R' is the radius of the nucleus assuming a uniform density and is related to R and c by

$$R'^2 = 5/3\ (.6R^2 + 7\Pi^2 C^2/5) \quad .$$

This condition assures that the minimum momentum transfer not exceed values for which the nucleus almost certainly breaks up. The number of intermediate states into which we divide the missing mass spectrum varies with energy and is shown in Table 1 along with the values used for the pp(nn) forward elastic scattering amplitude. We used the cutoff and increased the number of bins, or number of intermediate states at each energy to keep the grid size into which we divide the missing mass spectrum as fine as possible. Up to 60 gev/c the number of intermediate states we employ is approximately the same as the number used by Julius in his low energy calculation to all orders. In going to higher energies we increased the number of intermediate states only slightly because the amount of computing time required rises very rapidly with this number. The final result does not seem to be very sensitive to the number of intermediate states (as shown in some tests we conducted, and confirmed by more extensive tests [with $f_{ij} = 0$] reported to us by M.J. Longo in a private communication), but this is probably the major source of uncertainty in our calculation at the highest energies.

4.1.3 We list below the models we have calculated. The numbers correspond to the labels on the curves shown in Figure 5. The curves in Figure 5 having an "N" following the number were calculated with negative signs for all the non-elastic amplitudes (as discussed in Section 3.2.7). Of the curves shown, models 2,3,1N and 3N have not, to our knowledge, been calculated before.

Model 1 uses the prescription of Julius for all the forward amplitudes. This is given in Equation 21 . Our calculation duplicates that of Julius, except as we have noted, in the intermediate state mass spectrum.

Models 2,3 and 4 use the experimental missing mass spectrum Equation (22), to calculate the direct amplutides f_{1j} (and f_{j1}). The inter-resonance couplings, f_{ij} of model 2 are those used by Julius.

For model 3 we use the formula of Henyey, Equation (23), for the f_{ij}.

For model 4 we set the f_{ij} equal to zero. This means that each intermediate state diffractive resonance couples to itself and to the neutron, but not to any other resonances.

To illustrate the effect of the inelastic shadowing we show the curve for the unregenerated cross section, and to indicate the usefulness of this whole exercise we have included in Figure 5 all the available data in the energy range considered.

4.1.4. In as much as this is a theoretical investigation, we may perhaps be forgiven for not performing a rigorous error analysis. The fact is that for this calcualtion such an analysis is extremely difficult.

The heart of our calculation is the evaluation of Equations (9) and (16). From the numerical methods used we can determine that both these calculations give convergence more or less to within plotting accuracy. However the final result is dependent upon many experimental parameters which are used as inputs to the calculation, and upon several assumptions and approximations we have made along the way. Those listed in Section 2.2.1 have been discussed and justified. We feel that no substantial error is committed through our use of these assumptions.

As mentioned in Section 4.1.2 we found that our biggest source of uncertainty was in the convergence of σ_{ToT} with the number of intermediate states considered. Because of the expense in computing we were not able to investigate this point as thoroughly as possible. The indications are that the results could vary by perhaps 5 mb. or possibly more.

The curves we calculated are very sensitive to the nuclear and two-body scattering parameters which we use as input. Errors in these quantities are clearly reflected in the resultant cross sections.

Finally of course, the various models we use involve many different assumptions, but for the most part they stand or fall precisely on those assumptions. If the various considerations already listed do not contribute a significant error to the calculation, then the goodness of the models we use can be directly evaluated by how well they fit the data. We simply caution that in inspecting the various curves in Figure 5, the previous comments be kept in mind.

4.2. The Results-Discussion and Conclusions

Perhaps the most striking feature of Figure 5 is that models 3 and 3N are almost indistinguishable from model 4 which has no coupling between the different resonances($f_{ij} = 0$). The fact that this curve fits the data so well is compelling evidence for these couplings being small.

As we might have expected from the comments of Section 3.2.3, models 1 and 1N of Julius are very similar to the unregenerated cross section. That it gives such a poor fit to the data compels us to rule it out and reject Julius's suggestion that the inelastic shadowing is small. We conclude that the triple Regge formula, Equation (15), is not adequate to describe direct resonance production by neutrons on nucleons, at least not for small values of the missing mass. This conclusion is obvious from a glance at Figure 4.

Another interesting feature is the effect of negative non-elastic amplitudes on the various models. We note that for model 1 which uses Julius's form for the f_{ij}'s the effect is fairly marked, while for model 3 using Henyey's form the effect is somewhat smaller. This is in keeping with the fact that the f_{ij}'s are smaller in Henyey's model. We also note that at high energy the models with negative non-elastic amplitudes are all below the corresponding models with positive non-elastic amplitudes.

We also calculated model 2 with negative inter-resonance couplings (model 2N). This curve was found to lie very close to model 4 throughout the whole energy range calculated. Unfortunately to the accuracy we were able to afford in our computer calculation this particular model did not give convergence to plotting accuracy at the high energy end of our graph and so we omitted this curve. We feel however that model 2N, like models 3 and 3N is very difficult to distinguish from model 4 (although below 100 gev/c it lies between 5 and 10 mb. above the model 4 curve).

The fact that the data appears to be falling at 300 gev/c lends some support to model 3N. However the large error bars in the data, coupled with the ambiguities of the calculation make this the most tentative of conclusions. The fact that models 2N,3,3N and 4 remain close in their predictions even up to high energies make it seem rather unlikely that sufficiently accurate experiments can be performed to decide amongst them. For the time being then we really have little reason to suggest anything more complicated than model 4 ($f_{ij} = 0$).

APPENDIX A

We present here a proof due to Bochmann of the equivalence of the coupled channel optical model to a Glauber-type multiple scattering model. (NOTE: The notation used here, unless otherwise indicated, is the same as that of Chapter 2) As Bochmann notes, the Glauber production and multiple scattering formalism becomes very complicated if several production channels are present and multiple-step production processes are important. Also it is not applicable when longitudinal momentum transfer effects are important. On the other hand, while the coupled channel optical model formalism is easily applied, and does account for longitudinal momentum transfer, it is not easily justified. Therein lies the importance of the following proof.

Standard Glauber theory[3] tells us that after a wave function $\psi(\vec{r}) = e^{ipz}$ has passed through a potential it has the form $\psi(\vec{r}) = e^{ipz} S(\vec{b})$ where $S(\vec{b})$ is the scattering matrix, and

$$S(\vec{b}) = 1 - \Gamma(\vec{b}) \qquad \text{A-1}$$

with $\Gamma(\vec{b})$ being the profile function. We recall that

$$\Gamma(\vec{b}) = \frac{1}{2\pi i\, p} \int f(\vec{q}_\perp)\, e^{-i\vec{q}_\perp \cdot \vec{b}}\, d^2q_\perp \qquad \text{A-2}$$

For a wave passing through a nucleus Glauber assumes that the S matrix for the overall scattering is just the product of the individual S matrices, so that

$$S(\vec{b}_1,\ldots,\vec{b}_A;\vec{b}) = \prod_{n=1}^{A} S_n(\vec{b}_n-\vec{b}) \qquad \text{A-3}$$

where $\vec{b}$ is the impact parameter of the incident wave, and $\vec{b}_n$ is the transverse position of the n-th nucleon. (Since the S matrix can be written as the exponential of a phase shift, that is equivalent to saying that the overall phase shift is given by the sum of the phase shifts due to the individual nucleons)

From A-3 it follows that

$$\begin{aligned}\Gamma(\vec{b}_1,\ldots,\vec{b}_A;\vec{b}) &= 1-S(\vec{b}_1,\ldots,\vec{b}_A;\vec{b}) \\ &= 1-\prod_{n=1}^{A}\left[1-\Gamma_n(\vec{b}_n-\vec{b})\right] \qquad \text{A-4}\end{aligned}$$

This is the profile function for the instantaneous position of the nucleons and must be averaged over the nuclear density function.

Keeping in mind these facts from standard Glauber theory we proceed to Bochmann's proof. As before $f_{\beta\alpha}$ is the amplitude for (coherent) production of the state β by the state α incident on a nucleon. We now use Dirac notation and write the states as $|\alpha\rangle$, $|\beta\rangle$, etc., where we assume these states form a complete orthonormal set.

We define the two-body transition operator $\Gamma(\vec{r})$ with the matrix representation

$$<\beta|\ \Gamma(\vec{r})|\alpha> = \Gamma_{\beta\alpha}(\vec{r}) = \Gamma_{\beta\alpha}(\vec{b},z)$$

$$= \frac{1}{2\pi i\ p_\alpha} \int d^3q\ e^{-i\vec{q}\cdot\vec{r}} f_{\beta\alpha}(\vec{q}_\perp)\ \delta(q_z - q_L(\beta,\alpha)) \qquad \text{A-5}$$

where $q_L(\beta,\alpha)$ is the longitudinal momentum transfer between the states $|\beta>$ and $|\alpha>$.

$$\Gamma_{\beta\alpha}(\vec{b},z) = e^{-iq_L(\beta,\alpha)z}\,\Gamma'_{\beta\alpha}(\vec{b}) \qquad \text{A-6}$$

where $\Gamma'_{\beta\alpha}(\vec{b}) = \frac{1}{2\pi i p_\alpha} \int d^2q_\perp \quad e^{-\vec{q}_\perp\cdot\vec{b}} \ f_{\beta\alpha}(\vec{q}_\perp)$ A-7

So Γ is the 3-dimensional Fourier transform of the scattering amplitude, and Γ' is the 2-dimensional Fourier transform.

Following Glauber in assuming the product form for the S matrix (or additivity of phase shifts) we define the coherent production amplitude on a nucleus by

$$F_{\beta\alpha}(\vec{q}_\perp) = \frac{ip_\alpha}{2\pi} \int d^2b \quad e^{i\vec{q}_\perp\cdot\vec{b}} \{<\beta|\int d^3r_1 \ldots d^3r_A|u(\vec{r}_1,\ldots,\vec{r}_A)|^2$$

$$\prod_{i=1}^{A} [1-\Gamma(\vec{b}-\vec{b}_i,z_i)]\,|\alpha> -\delta_{\beta\alpha}\} \qquad \text{A-8}$$

where $\vec{r}_i$ is the position of the ith nucleon in the nucleus and $u(\vec{r}_1,\ldots,\vec{r}_A)$ is the normalized wave function of the nucleus in its ground state. We take the product in A-8 to be time-ordered. Since we assume that the incident high energy particle moves through the nucleus in the z-direction (without back-scattering) this is equivalent to taking a z-ordered product. The z-dependence of the $\Gamma(\vec{b}-\vec{b}_i,z_i)$ is given by A-6 and the remark that the function takes on its values for $z > z_i$ and is zero for $z < z_i$. To ensure that the incident wave has passed through the nucleus we shall shortly assume $z = \infty$.

We can simplify A-8 by introducing the operator

$$\phi'(b,z) = \int d^2r_1 \ldots d^3r_A |u(\vec{r}_1,\ldots,\vec{r}_A)|^2$$

$$\prod_{i=1}^{A} [1- \Gamma(\vec{b}-\vec{b}_i,z_i) \; \theta(z-z_i)] \qquad \text{A-9}$$

where $\theta(z)$ is the unit step function, i.e. $\theta(z) = 1$ for $z > 0$ and $\theta(z) = 0$ for $z < 0$. The product is still z-ordered. A-8 now becomes

$$F_{\beta\alpha}(\vec{q}_\perp) = \frac{ip_\alpha}{2\pi} \int d^2b \; e^{i\vec{q}_\perp \cdot \vec{b}} < \beta \,|\phi'(\vec{b},z = \infty)-1 > \qquad \text{A-10}$$

The problem of calculating $F_{\beta\alpha}$ is now reduced to that of calculating $\phi'(\vec{b},\infty)$ which we proceed to do. We note that A-9 gives us the initial condition $\phi'(\vec{b},z = -\infty) = 1$. We begin by differentiating A-9 with respect to z. Recall that the derivative of a step function is a Dirac δ-function, and that the z-dependence of $\Gamma(\vec{b}-\vec{b}_i,z_i)$ is contained in the exponential $e^{-iq_L z}$ and the step function. For the purpose of this differentiation however we invoke the coherence requirement $q_L z \ll 1$ to neglect the derivative of the exponential. Thus we have

$$\frac{\partial}{\partial z}\phi'(\vec{b},z) = -\sum_{j=1}^{A}\int d^3r_1 \ldots d^3r_A|u(\vec{r}_1,\ldots,\vec{r}_A|^2\,\delta(z-z_j)\Gamma(\vec{b}-\vec{b}_j,z_j)$$

$$\prod_{i\neq j}\left[1-\Gamma(\vec{b}-\vec{b}_i,z_i)\,\theta(z-z_i)\right] \qquad \text{A-11}$$

Since the integral in A-11 is independent of j we may write the equation as

$$\frac{\partial}{\partial z}\phi'(\vec{b},z) = -A\int d^3r_1 \ldots d^3r_A|u(\vec{r}_1,\ldots,\vec{r}_A|^2\,\delta(z-z_A)\Gamma(\vec{b}-\vec{b}_A,z)$$

$$\prod_{i=1}^{A-1}\left[1-\Gamma(\vec{b}-\vec{b}_i,z_i)\,\theta(z-z_i)\right] \qquad \text{A-12}$$

If we write $|u(\vec{r}_1,\ldots,\vec{r}_A)|^2$ as a product of single particle density functions (by neglecting correlations) so that

$$|u(\vec{r}_1,\ldots,\vec{r}_A)|^2 = \prod_{i=1}^{A}\rho(\vec{r}_i) \qquad \text{A-13}$$

then A-12 can be written as

$$\frac{\partial \phi'(\vec{b},z)}{\partial z} = (-A \int d^2 b_A \quad \rho(\vec{b}_A,z)\ \Gamma(\vec{b}-b_A,z)\ \phi'^{(A-1)}(\vec{b},z) \qquad \text{A-14}$$

where $\phi'^{(n)}$ is just the operator defined in A-9 for n nucleons. In particular $\phi'^{(A)} = \phi'$.

Equation A-14 becomes tractable by making the approximation $\phi'^{(A-1)} = \phi'^{(A)}$. This is a large nucleus approximation and creates an error of the order of 1/A, which is acceptable for large A.

We define the matrix element of $\phi'(\vec{b},z)$ by

$$< \beta\,|\phi'(\vec{b},z)|\alpha > = \phi_\beta(\vec{b},z) \ .$$

Taking the matrix element of A-14 and assuming the above approximation we get

$$\frac{\partial}{\partial z}\phi_\beta(\vec{b},z) = <\beta|(-A\int d^2 b_A \rho(\vec{b}_A,z)\Gamma(\vec{b}-\vec{b}_A,z) \quad \phi'(\vec{b},z)|\alpha >$$

$$= \sum_\gamma <\beta\,|\ (-A\int d^2 b_A \ \rho(\vec{b}_A,z)\Gamma(\vec{b}-\vec{b}_A,z)\ |\gamma><\gamma|\phi'(\vec{b},z)|\alpha >$$

$$= \sum_\gamma (-A\int d^2 b_A \ \rho(\vec{b}_A,z)e^{-izq_L(\beta,\gamma)} \ \Gamma'_{\beta\gamma}(\vec{b}-\vec{b}_A))\ \phi_\gamma(\vec{b},z)$$

A-15

where we have made use of Equation A-6 . If we define

$$u_{\beta\gamma}(\vec{b},z) = -2ip_\beta A \int d^2 b' \ \rho(\vec{b}',z)\ \Gamma'_{\beta\gamma}(\vec{b}-\vec{b}') \qquad \text{A-16}$$

and if we interpret $\phi_\beta(\vec{b},z)$ as in Equation 7 (Chapter 2) as the slowly varying part of the wave function, then A-15 may be written in the form

$$\frac{\partial \phi_\beta}{\partial z}(\vec{b},z) = \frac{1}{2ip_\beta} \sum_\gamma u_{\beta\gamma}(\vec{b},z)\, e^{izq_L(\beta,\gamma)}\, \phi_\gamma(\vec{b},z) \tag{A-17}$$

which we recognize as Equation(9) , the eikonal solution to the coupled channel optical model. This completes our proof.

REFERENCES

1. L. STODOLSKY, Herceg Novi Lectures 1969

2. (a) G.V. BOCHMANN and B. MARGOLIS, Nucl. Phys. B14 (1969)609
   (b) G.V. BOCHMANN, O. KOFOED-HANSON and B. MARGOLIS, Phys. Lett. 33B (1970) 222.
   (c) G.V. BOCHMANN, Ph.D. Thesis, McGill University (1971) Unpublished.

3. (a) The optical model solution for the eikonal approximation is presented in detail by Glauber in his famous lectures: R.J. GLAUBER, Lectures in Theoretical Physics, 1958 (Vol.1, P.315), Edited by W.E. Brittin and C.G. Dunham; (Interscience, New York, 1959).
   (b) See also K. GOTTFRIED, Optical Concepts in High-Energy Physics (CERN 72-20, Geneva, 1972). This is a set of lectures given in the CERN Summer Vacation Program, and provides a simple and concise summary of Glauber theory and coupled-channel calculations.

4. See for example G. BAYM, Lectures on Quantum Mechanics (W.A. Benjamin, Advanced Book Program, Reading, Mass. 1973).

5. E.A. ABERS, H. BURKHARDT, V.L. TEPLITZ and C. WILKIN, Nuovo Cimento 42 (1966) 365.

6. J. PUMPLIN and M. ROSS, Phys. Rev. Lett. 21(1968)1778.

7. V.N. GRIBOV, JETP (Sov.Phys.) 56 (1969) 892.

8. A.B. KAIDALOV and L.A. KONDRATYUK, Nucl. Phys. 856 (1973) 90.

9. V.A. KARMANOV and L.A. KONDRATYUK, ZhETF Pis.Red.18 (1973) 451; JETP Letters (Sov.Phys) 18 (1973) 266.

10. P.V. MURTHY et al., Nucl. Phys. B92 (1975)269.

11. D. JULIUS, Phys. Lett. 60B (1975) 58.

12. (a) We will not discuss triple Regge theory here. Excellent discussions of the subject along with references may be found for example in S. Humble, Introduction to Particle Production (Academic Press, London, 1974)
(b) D. HORN and F. ZACHARIASEN, Hadron Physics at very High Energies (W.A. Benjamin, Advanced Book Program, Reading, Mass. 1973).

13. P. FISHBANE and J. TREFIL, Phys. Rev. D5(1972)1222.

14. C.A. AYRE and M.J. LONGO, Phys. Lett. 62B (1976) 299.

15. The pp total cross sections were obtained by linearly interpolating the data of A.S. Carroll et al., Phys. Lett. 61B (1976) 303.

16. The ratio of the real to the imaginary part of the pp forward scattering amplitude was obtained from the graph of a dispersion relation calculated on the assumption that the pp total cross section increase indefinitely as $\ln^2 S$. The graph was presented by U. Amaldi in the Rapporteur's talk at the Second Aix-en-Provence International Conference on Elementary Particles, Aix-en-Provence, September,1973; this is available as a CERN preprint, entitled ELASTIC SCATTERING AND LOW MULTIPLICITIES.

17. H. ALVENSLEBEN et al., Phys. Rev. Lett. 24 (1970) 792.

18. See any text on numerical analysis, eg. F. Scheid, Theory and Problems of Numerical Analysis (Schaum's outline series, McGraw-Hill, New York, 1968).

19. G.V. BOCHMANN, Phys. Rev. D6 (1972) 1938.

20. E.F. PARKER et al., Phys. Lett. 31B (1970) 246.

21. J. ENGLER, et al., Phys. Lett. 28B (1968) 64.

22. J. ENGLER et al., Phys. Lett. 32B (1970) 716.

23. L.W. JONES et al., Phys. Lett. 36B (1971) 509.

24. T.P. McCORRISTON, Jr. UM HE 72-11, Ph.D. Thesis, University of Michigan, Unpublished.

25. P.V. MURTHY et al., Nucl. Phys. B92 (1975) 269.

26. J. BIEL, et al., Phys. Rev. Lett. 36 (1976) 1004.

TABLE I

P_{LAB} (Gev/c)	pp σ_{TOT} (mb)	$\rho = \frac{\text{Re } f(0)}{\text{Im } f(0)}$	Re f(0) (fm)	Im f(0) (fm)	No. of Intermediate States
5	39.28	-.34545	-2.7361	7.9203	4
10	39.14	-.27273	-4.30477	15.78414	4
20	38.87	-.21818	-6.840113	31.35052	4
30	38.60	-.18182	-8.49075	416.699	6
40	38.37	-.14545	-9.002834	61.8945	8
50	38.20	-.12727	-9.80322	77.0252	10
60	38.24	-.10909	-10.0939	92.5272	12
80	38.34	-.01818	-2.24895	123.6922	14
120	38.58	-.04545	-8.48635	186.6997	14
180	38.88	-.01455	-4.10512	282.227	16
240	39.21	+.00364	+1.38	379.4969	18
300	39.465	+.01818	+8.68102	477.4562	20
400	39.95	+.03636	+23.4339	644.432	20

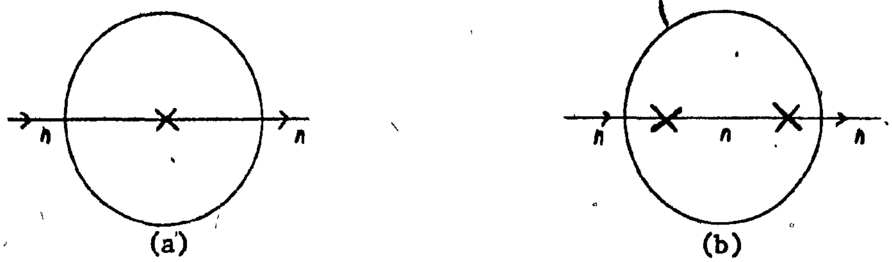

Fig. 1 -- One and two-step neutron elastic scattering.

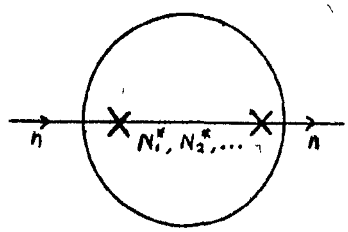

Fig. 2 -- Two-step neutron regeneration.

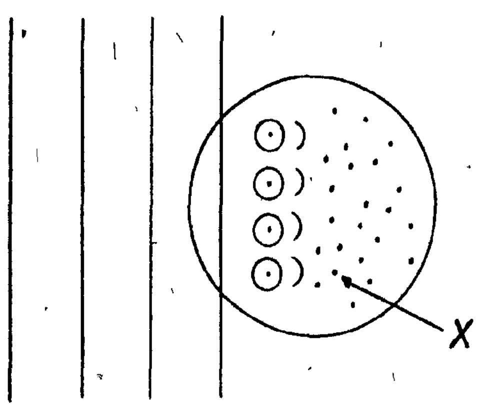

Fig. 3 -- Wave mechanical illustration of scattering.

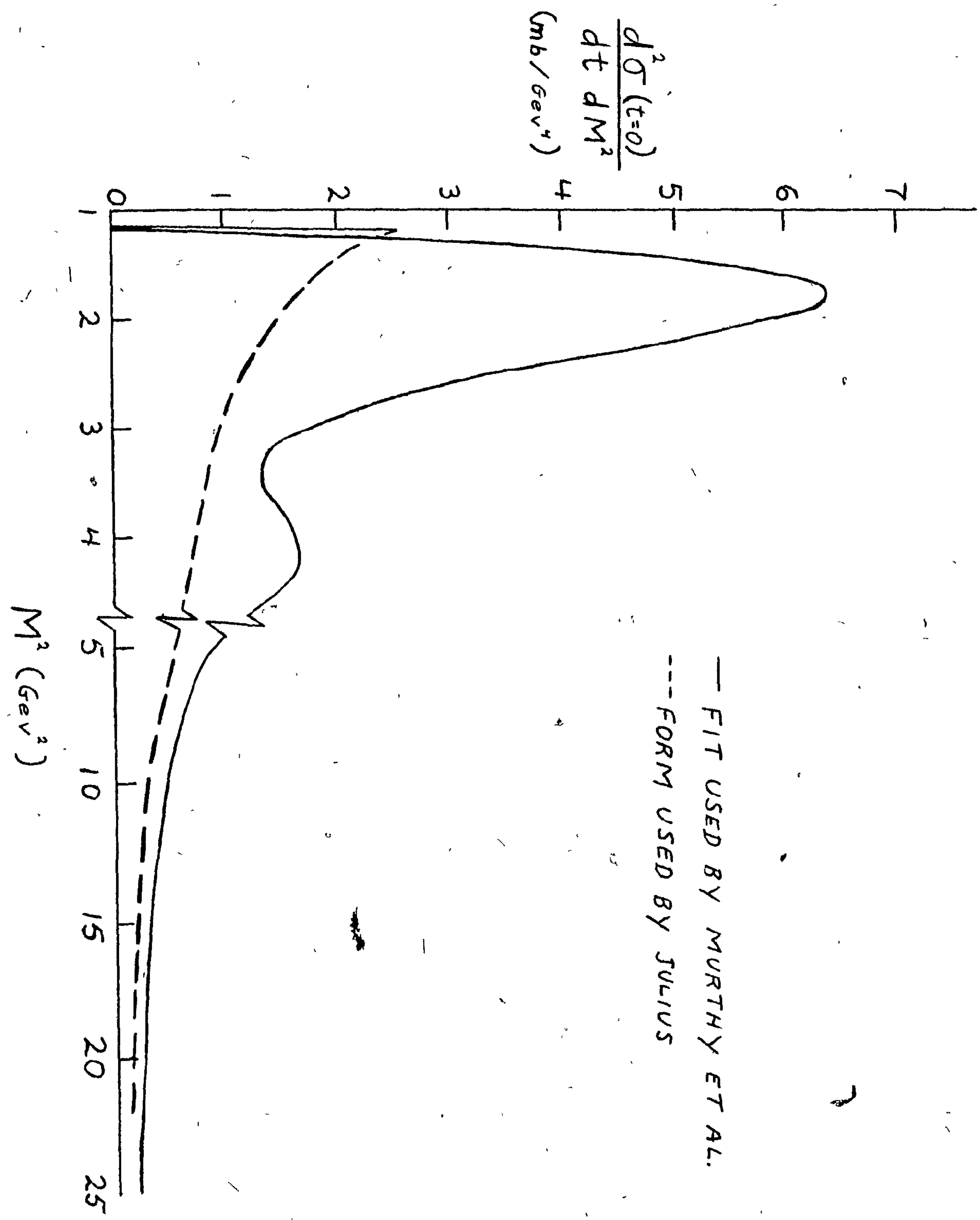

Fig. 4 -- A comparison between the form of $\frac{d^2\sigma(t=0)}{dt\ dM^2}$ used by Julius and the fit to the data used by Murthy et al.

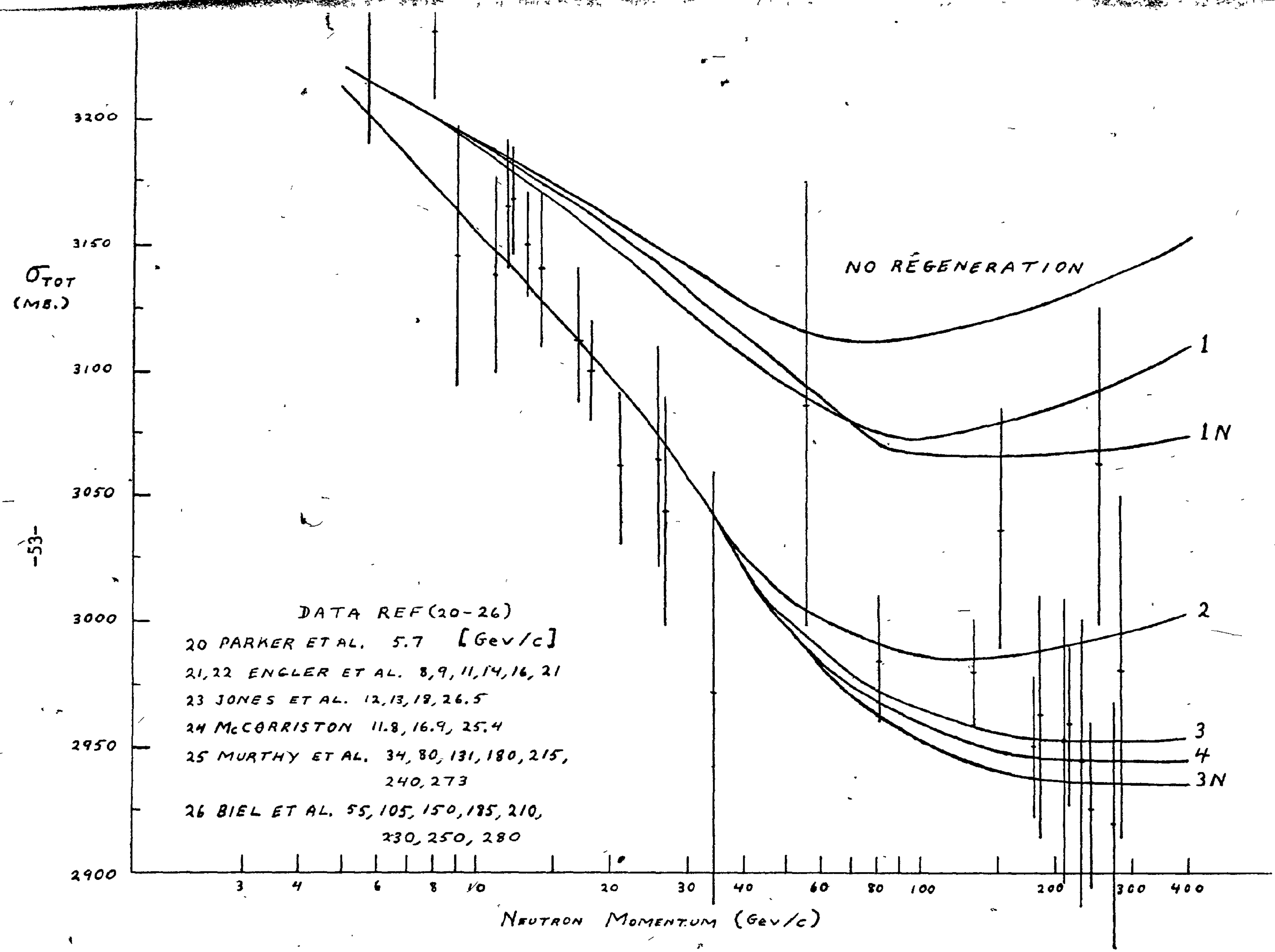

Fig. 5 — Neutron total cross sections on lead.